Scalable Yb-MOPA-driven carrier-envelope phase-stable few-cycle parametric amplifier at 1.5 μm

O. D. Mücke,[1,*] D. Sidorov,[1] P. Dombi,[1] A. Pugžlys,[1] A. Baltuška,[1] S. Ališauskas,[2] V. Smilgevičius,[2] J. Pocius,[3] L. Giniūnas,[3] R. Danielius,[3] and N. Forget[4]

[1]*Photonics Institute, Vienna University of Technology, Gusshausstrasse 27-387, A-1040 Vienna, Austria*
[2]*Laser Research Center, Vilnius University, Saulėtekio av. 10, LT-10223 Vilnius, Lithuania*
[3]*Light Conversion Ltd., P.O. Box 1485, Saulėtekio av. 10, LT-10223 Vilnius, Lithuania*
[4]*Fastlite, Bâtiment 403, Ecole Polytechnique, 91128 Palaiseau, France*
Corresponding author: oliver.muecke@tuwien.ac.at

Carrier-envelope phase-stable 4 μJ pulses at ~1.5 μm are obtained from a femtosecond Yb:KGW-MOPA-pumped two-stage optical parametric amplifier. This novel technology represents a highly attractive alternative to traditional Ti:sapphire front-ends for seeding multimillijoule-level optical parametric chirped-pulse amplifiers. For this task, we demonstrate stretching of the OPA output to ~40 ps and recompression to 33 fs pulse duration. As a stand-alone system, our tunable two-stage OPA might find numerous applications in time-resolved spectroscopy and micromachining. © 2009 Optical Society of America

OCIS codes: 320.7110, 190.4970.

Femtosecond optical parametric amplifiers (OPAs) have become versatile sources of ultrashort light pulses with pulse energies below a millijoule and wavelength tunability across the visible and IR spectral regions, which renders them ideal workhorses for numerous spectroscopic applications in physics, chemistry, and biology [1]. Taking advantage of the ultrabroad gain bandwidths in (noncollinear) parametric interactions, pulses with a duration much shorter than the pump pulses can be generated culminating in the demonstration of 4 fs pulses in the visible [2] and 8.5 fs pulses at 1.6 μm [3].

The vast majority of femtosecond OPA systems are pumped by the fundamental or second harmonic of complex expensive Ti:sapphire amplifier systems delivering millijoule-level ~100 fs pump pulses at kilohertz repetition rates [1–4]. Only recently, some research effort has been devoted to explore the potential of alternative pump sources for femtosecond OPAs beyond the traditional Ti:sapphire technology: For example, a frequency-doubled diode-pumped Yb:KYW oscillator with cavity dumping emitting 1.2 μJ 340 fs pulses at a 1 MHz repetition rate was used to pump femtosecond OPAs based on type-I β-barium borate (BBO) [5] or periodically poled lithium niobate (PPLN) crystals [6]. In [5], to achieve efficient white-light generation in a bulk sapphire plate for seeding the OPA, the 1.04 μm pulses needed to be spectrally broadened by self-phase modulation in a microstructure fiber and recompressed using dispersive mirrors. Another promising technology for pumping femtosecond OPAs are Yb-doped fiber-oscillator/(chirped-pulse) amplifier systems [7–11].

Here, we pursue a novel radically different technological path toward an intense tunable parametric femtosecond IR pulse source. The 130 μJ, 250 fs, 10 kHz output at 1.03 μm from a diode-pumped solid-state femtosecond Yb:KGW master–oscillator power amplifier (MOPA) system (Pharos, Light Conversion, Ltd.) is used to generate a white-light continuum seed that is subsequently amplified in two OPA stages yielding carrier-envelope phase (CEP) stable 4 μJ pulses tunable from 1.4 to 1.6 μm, which can be recompressed to a sub-40 fs pulse duration. Our system architecture has several highly attractive features. (1) With the advent of a mature 250 fs Yb:KGW MOPA it became possible to abandon complex expensive Ti:sapphire front-ends; (2) we avoid working close to the signal-idler wavelength degeneracy and reduce the quantum defect for the signal wave; (3) in the second OPA stage, we employ (nearly) collinear type II phase matching in potassium titanyl arsenate (KTA)/phosphate (KTP) that, as opposed to type I, supports a much narrower bandwidth but is free of parasitic self-diffraction [12]; (4) the Yb:KGW master oscillator, centered at 1.04 μm with a FWHM bandwidth of 30 nm, conveniently allows seeding of both the Yb:KGW power amplifier at 1.03 μm and Nd:YAG amplifiers at 1.064 μm for further upscaling of the pulse energy; (5) as discussed below, our scheme automatically results in passive CEP stability.

Although the two-stage OPA described in detail in this Letter can already be considered as a stand-alone system, intriguing for many applications in time-resolved spectroscopy and micromachining, the main objective of this Letter was the implementation of an elegant front-end for seeding an all-optically synchronized, (altogether) four-stage optical parametric chirped-pulse amplifier (OPCPA) [13], which employs a 100 mJ, 60 ps, 20 Hz, 1.064 μm Nd:YAG amplifier (Ekspla Ltd.) for pumping the power-amplification stages 3 and 4, finally delivering CEP-stable >10 mJ, ~40 fs pulses at ~1.5 μm [14]. Such a four-stage OPCPA system at 1.5 μm, which is beyond the scope of this Letter, will open the door to completely novel experiments in attosecond science.

The scheme of our two-stage OPA is depicted in Fig. 1. The 1.03 μm output from the femtosecond Yb:KGW MOPA is first split into two parts by means of a variable beam splitter (consisting of a half-wave plate and a thin-film polarizer); part one is used for
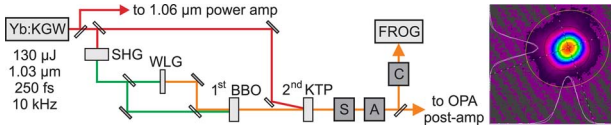
Fig. 1.   (Color online) Scheme of two-stage 1.5 μm OPA. Yb:KGW, 250 fs Yb:KGW MOPA system; SHG, second-harmonic generation in BBO; WLG, white-light generation in sapphire; S/C, grating stretcher/compressor; A, acousto-optic programmable dispersive filter. Right panel, far-field beam profile of second stage signal wave.

implementing the first OPA stage, part two is used for pumping the second OPA stage. In the first OPA stage, the 1.03 μm pulses are first frequency-doubled in a 1 mm thick type-I BBO crystal ($\theta=23.4°$, $\phi=90°$). Typically 8.5 μJ of 515 nm pulses are again split by a variable beam splitter into two parts: 1.3 μJ (measured behind a variable aperture used for fine-adjusting the input beam diameter) are focused onto a 10 mm thick sapphire plate using an 87 mm focusing lens. In the sapphire plate, a stable white-light (WL) continuum extending to wavelengths >840 nm [see Fig. 2(a)] is created in a single filament. For a sapphire plate thickness of 10 mm we obtain a stronger and more stable WL seed at >780 nm than for thinner plates of 4–6 mm. The WL continuum, which is recollimated with a 40 mm lens, is used to seed the first OPA stage. The WL seed pulses and the 515 nm pump pulses are combined collinearly (to avoid idler angular dispersion) on a dichroic beam splitter and both are focused onto a 4 mm thick type-I BBO crystal ($\theta=22.8°$, $\phi=90°$) with an $f=20$ cm spherical mirror to a $1/e^2$ pump beam diameter of 120 μm. In the pump beam, a variable aperture is used to adjust the pump energy to 1.4 μJ (thus, the parametric gain) and to minimize the detrimental effects of amplified spontaneous emission (ASE). By adjusting both the θ-angle of the BBO crystal and time delay between the seed and pump pulses, different wavelength re-

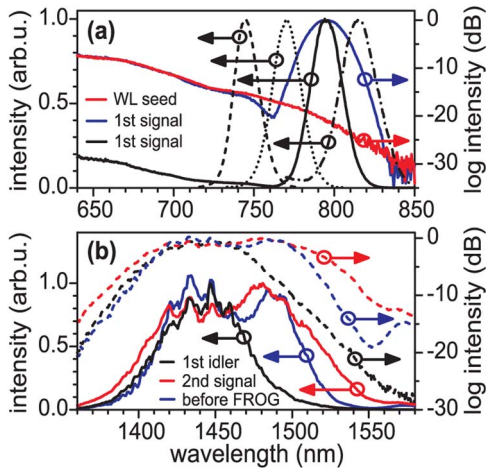

Fig. 2.   (Color online) Spectral properties of two-stage 1.5 μm OPA. (a) Near-IR WL seed and signal spectra of the first OPA stage. The dashed and dotted curves indicate tunability of the first stage signal (and idler). (b) IR CEP-stable seed, amplified second stage signal, spectrum before FROG setup. The amount of ASE is immeasurable in absence of the WL seed.

gions can be phase matched for efficient parametric amplification [see Fig. 2(a)]. In particular, selecting the ~795 nm wavelength for amplification, this configuration produces CEP-stable idler pulses [15] at 1.44 μm [Fig. 2(b)] that we use as a seed in the second OPA stage.

Following the pioneering work of Kraemer et $al.$ [16,17], we employ type-II KTP/KTA crystals (1.03 μm pump, ~1.5 μm signal, ~3.5 μm idler) for the second OPA stage (and subsequent power-amplification stages [14]) because these crystals (unlike borate crystals) are transparent for the mid-IR idler wavelength and exhibit a relatively broad bandwidth around 1.5 μm. The CEP-stable idler pulses from the first OPA stage are recollimated with a 10 cm lens and focused onto a 6 mm thick type-II KTP crystal ($\theta=45.5°$, $\phi=0°$) using a 50 cm lens. The pump beam is focused onto the same KTP crystal using a 100 cm lens under an (external) walk-off compensation angle of 2.1° with respect to the seed beam. For a pump beam diameter of ~550 μm measured at the KTP crystal input face and 69 μJ (measured behind a variable aperture) pump pulses, we achieve 4 μJ signal pulses, i.e., a pump-signal conversion efficiency of ~6% in the second OPA stage. The pulse-to-pulse intensity fluctuations of the two-stage OPA amounts to 2.5% rms noise, only two times larger than that of the Yb:KGW MOPA pump (1.2% rms). The far-field beam profile of the second stage signal wave shown in Fig. 1 is nearly Gaussian; the beam propagation factor was determined to be M^2 $=1.13\pm0.04$ as compared to $M^2<1.2$ of the pump.

The strong nonlinear optical Kerr effect in KTP/ KTA (nonlinear refractive index coefficient n_2(KTP/KTA)$=23.7\times10^{-16}$ cm^2/W as compared to n_2(BBO)$=2.9\times10^{-16}$ cm^2/W [18]) raises the important question, how severe is pump/idler-to-signal cross-phase modulation (XPM) in the second OPA stage and its effect on CEP stability. The nonlinear effects accumulated during the OPA process in a non-linear crystal of length L can be quantified by introducing a generalized B-integral

$$B = \frac{2\pi n_2}{\lambda_\text{s}} \int_0^L dz[I_\text{s}(z) + \gamma_\text{sp}I_\text{p}(z) + \gamma_\text{si}I_\text{i}(z)]. \quad (1)$$

The coefficients γ_sp and γ_si, which quantify the pump-signal and idler-signal coupling, are 2 for parallel polarizations and 2/3 for orthogonal polarizations [19]. For the three types of phase matching in OPAs, the values of γ_sp and γ_si, respectively, are (a) 2/3 and 2 for type I ($o_\text{s}+o_\text{i}\rightarrow e_\text{p}$), (b) 2 and 2/3 for type II ($e_\text{s}+o_\text{i}\rightarrow e_\text{p}$), and (c) 2/3 and 2/3 for type II ($o_\text{s}+e_\text{i}\rightarrow e_\text{p}$). Case (c) as used in our second OPA stage minimizes the detrimental XPM contribution of pump and idler on the signal wave.

CEP stability of the second OPA output was investigated by means of inline f-to-2f interferometry: a supercontinuum is generated by focusing the 1.5 μm pulses into a 3 mm thick sapphire plate with a 15 mm lens. After recollimation, the second harmonic of the 1.5 μm pulses is generated in a 0.2 mm thick
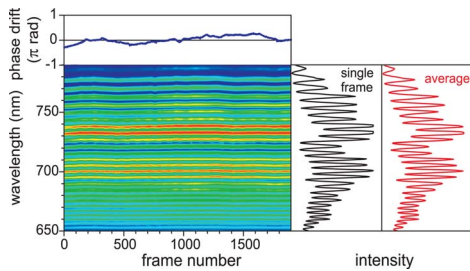
Fig. 3. (Color online) f-to-$2f$ interferograms of the second stage signal. The curves in the right panels indicate the average over 1900 frames (2 ms frame exposure time) and a single frame, respectively, on the same intensity axis. The above panel shows the extracted CEP drift.

type-I BBO crystal ($\theta = 19.8°$, $\phi = 90°$). With a polarizer, the supercontinuum and second harmonic generation (SHG) are projected onto a common axis and the resulting f-to-$2f$ interferograms from 650 to 790 nm are recorded with a spectrometer (see Fig. 3). The observation of stable interference fringes directly proves CEP stability and negligible influence of XPM on the CEP. The slow CEP drift observed in Fig. 3 is clearly of an environmental origin and can easily be compensated for by feedback stabilization of the interferometer formed by the seed- and pump-paths in the first stage (see Fig. 1).

In stand-alone applications of our two-stage amplifier, the well-behaved spectral phase of the second stage signal can readily be compensated for by highly reflective chirped mirrors. Here, keeping in mind mainly the development of a >10 mJ four-stage OPCPA system [14], we instead demonstrate that the second-stage output can be stretched to ~40 ps and again recompressed to a sub-40 fs duration using a grating-based stretcher/compressor pair (500 grooves/mm 69% efficient gold reflection gratings) [20] and an IR high-resolution acousto-optic programmable dispersive filter (DAZZLER). Figure 4 shows SHG-frequency-resolved optical gating (FROG) measurements of 1.47 μm pulses with a 92 nm FWHM bandwidth from the second OPA stage after stretching to ~40 ps and recompression to a FWHM 33 fs pulse duration. This result makes us confident that the >10 mJ output from the power-amplification stages, which exhibit similar spectral bandwidths [14], will be recompressible to comparable pulse durations.
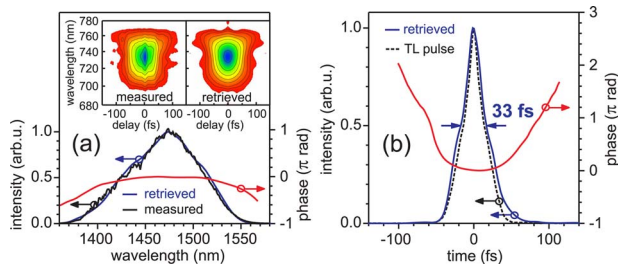

Fig. 4. (Color online) SHG-FROG characterization of stretched and recompressed 1.47 μm pulses. (a) Measured and retrieved spectrum, retrieved phase. The insets show the measured and retrieved FROG traces. (b) Retrieved temporal intensity and phase profiles indicating a FWHM 33 fs pulse duration. The transform-limited intensity profile corresponds to a 28 fs duration.

Our IR source, easily tunable in the 1.5–1.6 μm range, might find applications in pump–probe experiments on InAs quantum dot semiconductor optical amplifiers operating in the 1.55 μm telecommunications band or for buried-waveguide writing in semiconductors based on three-photon absorption.

References

1. G. Cerullo and S. De Silvestri, Rev. Sci. Instrum. **74**, 1 (2003).
2. A. Baltuška, T. Fuji, and T. Kobayashi, Opt. Lett. **27**, 306 (2002).
3. D. Brida, G. Cirmi, C. Manzoni, S. Bonora, P. Villoresi, S. De Silvestri, and G. Cerullo, Opt. Lett. **33**, 741 (2008).
4. E. Riedle, M. Beutter, S. Lochbrunner, J. Piel, S. Schenkl, S. Spörlein, and W. Zinth, Appl. Phys. B **71**, 457 (2000).
5. A. Killi, A. Steinmann, G. Palmer, U. Morgner, H. Bartelt, and J. Kobelke, Opt. Lett. **31**, 125 (2006).
6. M. Marangoni, R. Osellame, R. Ramponi, G. Cerullo, A. Steinmann, and U. Morgner, Opt. Lett. **32**, 1489 (2007).
7. C. Schriever, S. Lochbrunner, P. Krok, and E. Riedle, Opt. Lett. **33**, 192 (2008).
8. C. Homann, C. Schriever, P. Baum, and E. Riedle, Opt. Express **16**, 5746 (2008).
9. T. V. Andersen, O. Schmidt, C. Bruchmann, J. Limpert, C. Aguergaray, E. Cormier, and A. Tünnermann, Opt. Express **14**, 4765 (2006).
10. J. Rothhardt, S. Hädrich, D. N. Schimpf, J. Limpert, and A. Tünnermann, Opt. Express **15**, 16729 (2007).
11. J. Rothhardt, S. Hädrich, F. Röser, J. Limpert, and A. Tünnermann, Opt. Express **16**, 8981 (2008).
12. A. Varanavičius, A. Dubietis, A. Beržanskis, R. Danielius, and A. Piskarskas, Opt. Lett. **22**, 1603 (1997).
13. A. Dubietis, R. Butkus, and A. P. Piskarskas, IEEE J. Sel. Top. Quantum Electron. **12**, 163 (2006).
14. O. D. Mücke, D. Sidorov, P. Dombi, A. Pugžlys, S. Ališauskas, N. Forget, J. Pocius, L. Giniūnas, R. Danielius, and A. Baltuška, in *Ultrafast Phenomena XVI*, P. Corkum, K. Nelson, E. Riedle, R. Schoenlein, and S. De Silvestri, eds. (Springer, to be published).
15. A. Baltuška, T. Fuji, and T. Kobayashi, Phys. Rev. Lett. **88**, 133901 (2002).
16. D. Kraemer, R. Hua, M. L. Cowan, K. Franjic, and R. J. D. Miller, Opt. Lett. **31**, 981 (2005).
17. D. Kraemer, M. L. Cowan, R. Hua, K. Franjic, and R. J. D. Miller, J. Opt. Soc. Am. B **24**, 813 (2007).
18. W. Koechner, *Solid-State Laser Engineering*, 6th ed. (Springer, 2006).
19. G. P. Agrawal, *Nonlinear Fiber Optics*, 4th ed. (Academic, 2007).
20. M. P. Kalashnikov, E. Risse, H. Schönnagel, and W. Sandner, Opt. Lett. **30**, 923 (2005).